Deterioration of building materials in Roman catacombs: The influence of visitors

S. Sanchez-Moral[a], L. Luque[a], S. Cuezva[a], V. Soler[b], D. Benavente[c], L. Laiz[d], J.M. Gonzalez[d] and C. Saiz-Jimenez*[d]

[a]Departamento de Geologia, Museo Nacional de Ciencias Naturales (CSIC), Jose Gutierrez Abascal 2, 28006 Madrid, Spain
[b]Instituto de Productos Naturales y Agrobiologia de Canarias (CSIC), Avenida Astrofisico Francisco Sanchez 3, 38206 La Laguna, Spain
[c]Laboratorio de Petrologia Aplicada, Departamento de Ciencias de la Tierra y del Medio Ambiente, Universidad de Alicante, 03080 Alicante, Spain
[d]Instituto de Recursos Naturales y Agrobiologia de Sevilla (CSIC), Avenida Reina Mercedes 10, 41012 Sevilla, Spain

*corresponding author
fax: + 34 954 624002
Email: saiz@cica.es

Abstract

In the last decades, damages on building materials and mural paintings were observed in Roman catacombs. The damages were due to extensive formation of biofilms induced by artificial illumination and humidity. Microenvironmental data (temperature, CO_2 concentration, humidity, and atmospheric pressure) clearly showed the negative influence of visitors. Increasing heat, light and water vapour condensation into corridors and cubicles favoured biofilm development. The composition of biofilms were different and depended mainly on distance to illumination sources and humidity, thus denoting the influence of light on the growth of phototrophic microorganisms in the catacombs. In addition, biofilm distribution was governed by the type of material to be colonised. This study shows that countermeasures are needed to prevent deterioration of hypogean environments.

Keywords: Bioreceptivity, volcanic rock, building materials, biodeterioration, biofilm, microenvironment, Roman catacombs

Introduction

Microorganisms inhabit all possible biosphere environments including natural and man-made hypogean environments. Hypogean environments show a great stability (constant humidity and temperature), and the abundance of nutrients, when combined with the presence of artificial illumination, provide a suitable niche for phototrophic microorganisms. These microrganisms play a significant role in geological processes and influence biogeochemical cycles (Ehrlich, 1998).

Roman catacombs are hypogean monuments included in a tourism net that brings more than 500.000 visitors per year. Areas receiving visits are exposed to intense modifications both because of visitors and conditioning of the galleries for visits (i.e., lamps, ventilation, openings to the exterior, doors and panels, etc.). These factors result in conspicuous biofilm distributions covering mural paintings, walls and ceilings that contrast with areas restricted to visitors in which biofilms were not observed.

Cyanobacteria are photosynthetic microorganisms that can use CO_2 as a carbon source for growth. Due to their peculiar ability to adapt to extremely low photon flux densities and to a variety of spectral emissions, cyanobacteria are the major organisms responsible for biofilm formation in catacombs (Albertano et al. 2003). Heterotrophic bacteria, a few green algae, diatoms, and mosses were also associated to cyanobacterial biofilms (Albertano and Urzì, 1999). Damages induced by biofilms were observed on corridors, tombs and crypts or cubicles, threatening the conservation of this valuable cultural heritage.

In a study carried out in two Roman catacombs, Saint Callixtus and Domitilla, both microenvironmental conditions and rock and artificial building materials were investigated in order to determine the influence of visitors.

Materials and methods

Sampling and sample location

The catacombs were built between the second and seventh century AD and are considered among the greatest and most important Roman monuments. Saint Callixtus Catacombs are part of a cemeterial complex with a network of galleries about 20 km long, distributed in four levels, and with a depth of more than 20 metres. Domitilla Catacombs are spread over 15 kilometres of underground caves some of which are inaccessible, and distributed in three different levels. Due to the extensive period of construction of the catacombs, differences in mineralogical and textural composition of mortars, stuccos and bricks were observed.

After a survey campaign in 2001, a set of rocks, artificial building materials and microbial mat (biofilm) samples were collected from the two catacombs at eight locations. More than 40 samples from different areas were collected aseptically using scalpels, small chisels, and hammer and kept in hermetic plastic bags or acrylate boxes for geological studies. Special attention was addressed to the areas colonised by microorganisms. Biofilm samples were kept in sterile tubes at 4°C for two days until processed in the laboratory. These samples were collected on different type of materials, taking into account distance to lamps, humidity and type (colour) of biofilm.

Petrographical techniques

Aliquots of different samples were observed under a stereomicroscope, with light guides and halogen bulb, to separate their different layers for subsequent analysis. Optical observation of small chips of samples cut-polished up to 35 micrometers in thickness were performed in a polarising transmission light microscope, Nikon Eclipse C 600 POL, equipped with a digital camera Nikon Coolpix 950 for identification of the mineralogy and type of porosity, cracking, secondary mineral formation and binder/aggregate ratios in mortars. Morphology, textures, relationships, composition, crystal shapes and sizes of different materials were also studied by scanning electron microscopy (SEM) in a Philips XL20 SEM and environmental scanning electron microscopy (ESEM) in a Philips XL30/40 ESEM-EDS Oxford-WDS. Samples for SEM studies were metallized using gold vapour under vacuum (50 Å of gold cover) in a Bio-Rad SC515 sputter coating unit and observed at accelerating voltages of 20-30 kV. EDS analyses were obtained using a Phillips EDAX PV9900 with a light element detector type ECON.

Petrophysical techniques

Total open porosity, pore size distribution and superficial specific area were characterised using mercury intrusion porosimetry (MIP) technique, nitrogen absorption technique and helium pyknometer. Connected porosity (P_{conc}), pore size distribution, median pore size (r_m) and bulk density (ρ_{bulk}) were obtained in an Autopore IV 9500 Micrometics mercury porosimeter. Pore size interval characterisation by MIP ranges from 0.002 to 200 μm, which corresponds to the highest and the lowest head pressures, respectively.

In order to quantify porosity fraction below 0.002 μm, which can not be measured by MIP, total porosity was calculated. Total porosity (P_T) includes open porosity and close porosity. Open porosity is the volume of pores accessible to any given molecule, and close porosity is the volume of isolated pores dispersed over the medium. It is important to mention here that connected porosity is the volume of pores accessible to a given molecule and depends on the used technique. Consequently, connected porosity is a fraction of the total open porosity. Total porosity was calculated as follows:

$$P_T(\%) = \left(1 - \frac{\rho_b}{\rho_t}\right) \cdot 100 ,$$

where ρ_t is the true density which is defined as the ratio of its mass to solid volume.

True density was obtained by an AccuPyc 1330 Helium pyknometer. Bulk density of a material is defined as the mass to volume ratio, including the volume of voids and solid. It may be estimated by mercury porosimetry to lowest head pressure (0.0030 MPa). Therefore, total porosity was calculated by the combination of mercury porosimetry and helium pyknometry data.

The determination of specific surface area (SSA), which is defined as the interstitial surface area of the voids and pores per unit mass of the porous material, was accomplished by means of nitrogen absorption. The determination of SSA was carried out through the BET methods, analysing the points in the relative pressure interval P/P0 = 0.1 – 0.35 by an Autosorb-6B Quantachrome equipment.

Chemical and mineralogical analyses

Chemical composition of samples was obtained by Inductively Coupled Plasma Mass Spectrometer (ICPM) for trace elements, and atomic absorption spectroscopy (AAS) for major and minor elements. The concentration of ferrous iron was determined by wet chemistry with a redox titration using ceric sulphate as titrant and measured in the endpoint with an ORP electrode. The semi-quantitative mineral composition of different materials was determined by X-ray diffraction (XRD) using a Phillips PW-1710 powder diffractometer with CuKα radiation.

Microclimate measurement system

Characterisation of hypogean microenvironmental parameters was carried out by means of an automated data recording system installed from March 2002 to March 2003 in the Crypt of Oceanus (Saint Callixtus Catacombs), so called after the mythical personification of the sea painted on the vault. This crypt is modest in size (3 x 3 m) and decorated with strongly marked red bands. The monitoring system consisted of the combination of sensors, signal conditioning and data logger for the recording and storage of data at predetermined intervals of time (usually each two minutes) (Sanchez-Moral et al. 2004b). The monitored environmental parameters were atmospheric pressure, temperature (inside the catacomb, external air, rock, and lamp), air CO_2 concentration and air relative humidity.

Composition of biofilms

DNA was extracted from minute biofilm samples using the NucleoSpin Food DNA extraction kit (Mackerey-Nagel, Düren, Germany). Amplification of 16S rRNA gene sequences was performed by PCR using bacteria- or cyanobacteria-specific primers. Bacterial primers were 27F and 1522R according to Edwards et al. (1989). Cyanobacterial primers were Cya106F and Cya781R (Nübel et al. 1997). PCR conditions were 95ºC for 2 min, followed by 35 cycles of 95ºC 15s, 55ºC 15 s, and 72ºC 2 min; the reaction finished with a step at 72ºC for 10 min. Bacterial diversity was visualized by Denaturing Gradient Gel Electroporesis (DGGE) (Muyzer et al. 1993). Cloning of PCR products was carried out with a TOPO-TA cloning kit (Invitrogen, Carlsbad, USA) according to the manufacturer´s recommendations. Clone screenings were performed as described by Gonzalez et al. (2003). Sequence analysis was performed by homology search using the BLAST algorithm (Altschul et al. 1990) at the National Center for Biotechnology Information (NCBI; http://www.ncbi.nlm.nih.gov/BLAST/).

Results

The catacombs are composed of six main types of materials (Figure 1) with different geochemical, mineral and textural properties:

- Coarse-grained tuff
- Fine-grained tuff
- Mortars. Artificial mixture of tuff fragments in a carbonate cement
- Plaster/stucco. Mixtures of calcite, zeolites and special clays
- Bricks. Mixture of feldspars, clays and quartz sands, prepared by heating to high temperature
- Marble. Well re-crystallized calcite and dolomite

Table 1 shows the chemical composition, mineral composition and porosity of five of these materials. Only two micro-samples of detached marble were collected

because this material was part of statues, tombs and other valuables assets. In Table 1 bulk (ρ_{bulk}) and true (ρ_{true}) density, total porosity (P_T), mean radius (r_m) and SSA were also included.

The high total porosity of different materials, excepting marbles (<1%), is remarkable. Total porosity ranges from 37% in stuccos to 70% in coarse tuff. This could favour both infiltration of waters enriched in nitrates originated at the agricultural soils above the catacombs and retention of condensation waters on their surface. In this context, there were very scarce dripping water points in the two studied catacombs. Two water samples showed a moderate concentration of NO_3^- (46 mg/L) and SO_4^{2-} (34 mg/L) (Sanchez-Moral et al. 2004a).

Volcanic rocks, mortars and stuccos were quantitatively the most abundant materials, while bricks and marbles had a more restricted use. The analysed materials were rich in silica, aluminium, iron, calcium and magnesium among the major elements. In addition, they showed high contents in trace elements. All of them presented a high total porosity (Figures 2 and 3). Petrographic characterisation showed that close porosity of the studied materials was small; therefore, total porosity may be considered equivalent to open porosity. SSA of the materials was variable and directly related to porosity and inversely related to pore size. Low values of porosity lead to low values of SSA (for example, stuccos). Materials with high porosity but small mean pore size (for example, fine tuff) presented a higher SSA than materials with a large mean pore radius and smaller porosity (for example, coarse tuff).

Volcanic rocks

Physical and chemical characterisation of volcanic rocks revealed that the host rock of catacombs consisted on different episodes of volcanoclastic fall deposits from Colli Albani eruptive succession disposed in thick layers. The galleries constituting both Domitilla and Saint Callixtus Catacombs were dug in fairly consolidated layers of fine-grained tuff while hardened deposits of coarse-grained tuff were used as support elements (ceilings, walls). Both deposits were tuffs and the so-called pozzuolana (scoriae in an ash matrix) of alkaline composition.

Primary or early diagenetic minerals constituents of pozzuolana were mainly aluminum silicates such as phyllosilicates (illite, biotite) and feldspars (orthoclase-Ba, sanidine) as principal components of fine tuff, and analcime and pyroxenes (augite-aegirine) as major constituents of coarse tuff, disposed in an abundant vitreous (volcanic glass) matrix. Volcanic glass is highly susceptible of being altered and its typical secondary products were clays and zeolites (analcime). Porous system of the two differentiated rock types was very different; fine-grained tuff showed very low median pore size and thus high specific surface area, while coarse-grained tuff presented opposed characteristics. Total and connected porosity in coarse-grained tuff were quite higher than in fine-grained tuff.

Chemical composition of the bulk rock was characterised by high amount of SiO_2 (42-48 wt%), Al_2O3 (15-20 wt%), CaO (5-10 wt%), Fe_2O_3-FeO (5-10 wt%), Na_2O (0.5-5 wt%), MgO (1-3 wt%), K_2O (0.5-2 wt%) and P_20_5 (0.1-1%) as major elements. Among the trace elements, Ba and Sr were the most abundant rock constituents, ranging from 1200 to 7200 ppm and from 400 to 3000 ppm, respectively. Specific analyses by means of EDS revealed that volcanic glass had similar chemical composition to bulk rock, but with a higher content of phosphorus. Coarse tuffs showed higher contents of Ca and Na than fine-grained tuffs but, on the contrary, presented smaller concentrations of potassium, manganese and the trace elements analysed.

Building materials

Artificial building materials cover extensive areas of the walls and ceilings, mostly with a decorative purpose. These materials were usually a mixture of tuff fragments in a carbonated matrix forming a mortar and a thin layer of slaked lime or stucco commonly decorated with frescos (Figure 3).

The Roman mortar or concrete consisted of a mixture of fragments of local volcanic rock (aggregate) with lime putty (binder) and water. The mixture reacted and conferred an enormous resistance to this building material allowing these two thousand years old monuments to be still functional. After mixing, lime converted to calcite due to CO_2 supply from the atmosphere. Mortars in the catacombs were not used as structural framework but for covering ceilings and walls to avoid detachment of rock fragments and subsequent decoration of tombs and crypts.

The chemical and mineral compositions of the studied mortars were quite homogeneous and usually corresponded to the preferable use of fragments of coarse-grained tuff as aggregate and a calcium-carbonate cement. The most remarkable feature was its high content of copper in comparison with the rest of the materials. The structure of these mortars showed: (i) coarse aggregates and thick beds in the inner side, (ii) thin, smoothed, light, and fine-grained external surfaces with low content of aggregates, and (iii) paintings and frescos over stuccos in the outer (Figure 2). The high porosity of these mortars can be attributed to fast hardening in a CO_2-enriched environment. Frequently, a former thin layer of pure lime was extended onto the soft and crumbly natural surface of the host rock (Figure 3).

Stucco is a special mortar made of slaked lime as binder, mixing water, and quartz grains or volcanic rock fragments as fine aggregate. Therefore, stucco surface, at the end of the hardening process, contained almost exclusively calcium carbonate with minor fine aggregates (Figure 3). It stands out the sporadic presence of some amounts of gypsum ($CaSO_4 \cdot 2H_2O$) without any specific and strict proportion in the studied samples. The stuccos showed the smallest total porosity and very low values of SSA (6.6 m^2/g). However, stuccos had the highest median pore size related to cracking of the paste after retraction because of drying and further changes in volume.

Other materials used in catacombs both for structural and decorating purposes were bricks and marbles. The sampled bricks consisted of clays, mixing calcareous water, feldspars and quartz, burnt in the kiln. In Domitilla Catacombs, quartz and albite together with clays were the main constituents of the mixture. Bricks from Saint Callixtus Catacombs showed a high proportion of calcium carbonate, and quartz was absent. All studied bricks had a very compact structure, resistant to deterioration, probably related with its low SSA values (1.9 m^2/g) in spite of its high total porosity. Its main use as structural component of the catacombs contributed to the great durability of the whole construction.

Marbles were well re-crystallised carbonate material (98% calcite, 2% dolomite) with low porosity (< 1%), commonly used as tombstones, columns and friezes, and often decorated with engravings.

Material decay

Material decay was locally intense in Saint Callixtus and Domitilla Catacombs. Mechanical differences between soft and porous volcanic host rock and its rigid slight permeable calcareous coating gave rise to locally extensive crumbling and decay of the walls in Roman catacombs. ESEM and thin section analysis showed that these mechanical processes were due to its high porosity and lost of coherence, as a consequence of previous geochemical alteration of the rock. Recent inorganic geochemical processes such as dissolution or corrosion were rare on artificial materials. In some cases, small mechanical fissures or initial porosity seems to be enlarged by dissolution of mortar and stucco internal surfaces. In theses cases, calcite crystals were partially dissolved. Older processes such as geochemical dissolution and mineralogical transformation of the host rock were common, as we can deduce from textural, geochemical and mineralogical features.

Biogenic deterioration was observed (Figure 4). Micropits and mineral dissolution and later crystal aggregate formation were evidenced mainly in some calcareous surfaces. These processes were not very extensive and were related with large biofilms coating the material (Figure 4A). On the other hand, bio-precipitation was widely observed on different materials. The identified biominerals were calcite coating around cyanobacteria sheaths (Figure 4B), a dense net of needle-like calcite crystals (Figure 4E), vaterite spherules (Figure 4H), barite fibres and calcite regrowth on surfaces and previous biogenic crystals (Sanchez-Moral et al. 2003b). The most conspicuous biomineral accumulation was located in white biofilm-material interface, where intense geochemical reactions occur (Sanchez-Moral et al. 2004a). White biofilms are mainly formed by actinobacteria and their filaments penetrate the materials thus forming a dense network of hyphae beneath the surface contributing to chemical dissolution and pitting formation.

Capability of catacomb's bacteria and cyanobacteria to produce mineral precipitates has been previously demonstrated in laboratory cultures (Sanchez-

Moral et al. 2003a). These bio-precipitates usually consists on calcium carbonate polymorphs (calcite, aragonite, varite) but other compounds like sulphates or phosphates have also been found both in cultures and natural environments (Sanchez-Moral et al. 2003b, 2004a). Biogenic mineralization arise from previous organic and inorganic dissolution of the material (both volcanic and calcareous) and later precipitation due to changes in chemistry of the bulk solution or around microbial membranes. Carbonates show affinity by organic compounds and calcium tends to joint to cellular membranes giving rise to inorganic mineral precipitation on them (Buczynski and Chafetz, 1991). With the exception of barite formation (Sanchez-Moral et al. 2004a) that seems to be linked to volcanic glasses rich in barium and phosphorous, no differences have been observed between biominerals formed on different materials.

In addition to biogenic decay processes, aesthetic damage was observed, due to biofilm coverage over frescos and paintings.

Microclimate

In Figure 5A values of temperature, humidity and CO_2 taken during an annual cycle in the Oceanus crypt (Saint Callixtus Catacombs) are shown. Temperature was around 17-18ºC at the first stage of the study, but nowadays it oscillates much more, descending even to 11ºC due to recent changes in the artificial ventilation system that increased external weather influence. CO_2 concentration was quite high, ranging from 500 to 3500 ppmv, being higher in Domitilla than in Saint Callixtus Catacombs.

As can be observed in Figure 5A, curve profile looks very sawed and irregular. It was due to the effect of the visitors on the environment. In Figure 5B this effect was clearly visible along three days; the first and the last one with tourism activity and the second one corresponding to a day without visits. The sharp temperature increase was due to the automatic ignition of lamps when people passed along the corridors, and to human corporal heat. CO_2 also increased significantly due to breathing. Quantification of relative and absolute humidity was very difficult, due to its value very close to saturation ($\geq$ 95%). Temperature sensors installed in air and different materials indicated that temperature of rock and mortars was always lower than air temperature, inducing, consequently, water condensation on material surfaces (Figure 5C).

Biofilm distribution

The observation of biological colonisation in the catacombs and the analysis of samples from different areas indicated that biofilms can be initially classified according to their colour. This was the most conspicuous difference found in catacomb walls and ceilings where two main types of biofilms, green and white, can be distinguished. Biofilm colour reflects the abundance of the phototrophic microorganisms.

In general, biofilms developed mainly in areas accessible for visitors (Figure 6) and not over the extensive surfaces of tombs and corridors out of tourist circuits. Table 2 shows a model of their distribution on the basis of distance to lamps and type of material.

At the entrance and in artificially illuminated areas, phototrophic microorganisms (cyanobacteria) were very abundant and they were distributed as patches of a green biofilm over a great extension of the material surface (Figure 6A). The biofilms were constituted by abundant exopolymeric substances (EPS) that comprised a mass ranging from 150 to 200 μm thick covering the whole surface of materials. Diatoms were very abundant in lighted areas (Figure 4C) and sometimes covered by EPS or grouped inside EPS holes and irregularities. The cyanobacterium *Scytonema julianum* was covered by mineral calcification forming a calcified sheath (Figure 4B) and usually accompanied by filamentous bacteria (Figure 4D).

White biofilms were distributed in patches on different materials, although they extensively coated volcanic rock, preferably fine-grained tuff, in lighted and wet ceilings of corridors and tombs, or in gallery and niche ceilings where water easily condenses (Figure 6B). These biofilms were mainly formed by actinobacteria. Where biofilm development was maximum, it was separated from the material by a thin aerial interface (Figure 4E). The living biofilm consisted mainly on a network of filamentous microorganisms (Figure 4F) with scarce EPS. The internal zone showed interwoven microorganisms (Figures 4G,H) and a thin layer of EPS. Interface was hollow and some cocci and bacilli as well as thin filamentous actinobacteria were observed. White biofilm distribution depended not only on light intensity but also on humidity since this type of biofilm was best developed on wet rock surfaces of visited areas and in patches concentrated in wall hollows.

In addition, brown biofilms were also observed. This colour likely indicates some necrotical cyanobacterial status. These biofilms were commonly associated to well illuminated areas and developed predominantly on calcareous materials (stuccos). Brown biofilms reached a limited extension around sources of illumination. They were constituted by abundant EPS that comprised a mass ranging from 50 to 200 μm thick covering the whole surface of materials.

In most places changes of biofilm types occurred between 0.6 and 1.2 m from the lamps, showing a clear gradation from green to white depending on the distance (Table 2). At less than 0.6 m the materials appeared dry or almost dry and hot when lamps were lit. In the proximity of the lamps, strong changes of temperature and humidity take place, being detected intense condensation processes when turning off the lighting. At this distance, maximum development of green biofilms with some patches of black to brown colour was observed. At 0.6 m outward from the lamp green biofilms decreased and mixed with white biofilms. From 0.8 to 1 m only white biofilms were evident. In catacomb walls, 1 m distance from the lamps means low light incidence and a cool and wet environment. EPS, biofilm thickness

and surface coverage were drastically reduced 1 m from lamp outward. This was generally the case with the exception of areas with well or moderate lighting and intense water condensation, i. e. high ceilings in corridors, where white biofilms were still very dominant. Under these conditions a dense coating of white biofilm formed a continuous coverage mainly developing mainly on volcanic rocks.

At approximately 1 to 1.5 m from the light sources, biofilms were not visible or scarce on dry surfaces and its thickness decreases to less than 25 μm when present. As biofilms were thinner far from light, mineralization was associated, sometimes mixed with broken diatom siliceous structures.

Bricks and marbles were usually not colonised and only rarely bricks were coated by a less dense biofilm.

Community members

By comparing DGGE analysis from green, white, and brown biofilm samples, common bands to each biofilm type were detected (Figure 7) In green biofilms bacterial and cyanobacterial sequences were detected. Among the cyanobacteria, sequences of the genera *Cyanothece*, *Phormidium*, *Cyanobacterium*, *Aphanothece*, *Gloeothece* and uncultured cyanobacteria were identified. *Gloeothece* sequence was only detected in a sample corresponding to Saint Cecily tomb (Domitilla Catacombs). Identified bacteria included the genera: *Aquabacterium*, *Teichococcus*, *Devosia*, *Alcaligenes*, and uncultured bacteria belonging to the groups Verrucomicrobia and Acidobacteriales, as well as unidentified gamma- and alpha-Proteobacteria. In white biofilms, sequences corresponding to the *Cyanobacterium*, *Cyanothece*, *Synechococcus,* *Leptolyngbya*, and *Nitrospira* genera were detected as well as other unidentified cyanobacteria. The bacterial genera found in white biofilms were: *Hydrocarbophaga*, *Sporichthya*, *Blastochloris*, *Pseudonocardia*, *Actinobispora*, *Frankia,* *Nordella*, *Virgosporangium*, and *Pelobacter*, and uncultured alpha-Proteobacteria and several unidentified bacteria. From brown biofilms sequences of the cyanobacterium *Scytonema hofmanni*, and species of *Cyanobacterium*, *Cyanothece*, *Leptolyngbya*, *Synechococcus,* and an unidentified cyanobacterium were detected. Bacteria detected in brown biofilms were *Variovorax paradoxus*, and species of the genera *Xanthomonas*, *Phyllobacterium*, *Hydrocarbophaga*, *Agromyces*, *Nordella*, *Pedomicrobium*, *Brevundimonas*, uncultured bacteria belonging to the Acidobacteriales, and other unidentified bacteria.

Discussion

The susceptibility of a material to be colonised by one or several groups of living organisms or “bioreceptivity” (Guillitte, 1995) depends on environmental factors, such as water availability, pH, climatic exposure, nutrient sources, and on petrologic parameters, such as mineral composition, type of cement as well as

porosity and permeability of the rock material (Ariño and Saiz-Jimenez, 1996; Warscheid and Braams, 2000).

Dim light habitats like the catacombs are characterized by the development of terrestrial epilithic cyanobacteria and few eukaryotic algae developing along light gradients. The capability of cyanobacteria and other phototrophs of adapting to varying light conditions is well-known and at very low irradiance cyanobacteria have lower light requirements and outcompete other phototrophic organisms. In the catacombs two types of lamps are used: incandescent lamps covering from the blue to the red zones of the visible spectrum (absorbed by chlorophyll), and fluorescent ones with major peaks in the green and orange part of the visible spectrum (absorbed by their phycobiliproteins). Both lamps promote the growth of phototrophic microorganisms.

On the basis of biofilm distribution we can deduce that microenvironmental changes induced by visitors and tourism infrastructures favoured microorganisms colonization. Analytical data and in situ observations revealed that the type of biofilm and its density was clearly determined by environmental parameters and material characteristics. Illumination sources, even at the low intensities existing in the catacombs, explained the presence of significant communities of phototrophic microorganisms (mainly cyanobacteria) which produced aesthetic, physical and chemical damages.

Besides the evident influence of light in distribution of phototrophic microorganisms, biofilms showed preference for different type of materials. In this sense, two main groups of colonized materials were distinguished: calcareous related with artificial building materials, and volcanic formed by the host rock dug to build catacombs. All the analysed materials were relatively homogeneous in chemical composition but showed some important differences concerning concentration in calcium carbonate and minor and trace elements. In fact, lime stuccos showed the highest concentration of calcium, carbonate, molybdenum and phosphorus. Molybdenum, essential for nitrogen fixation and metabolism, is not very abundant in other catacomb materials, while phosphorus is also abundant in volcanic glasses. It can influence microbial preferences for colonization, cyanobacteria composition of biofilms or community structure (Keinänen et al. 2002). Under similar light conditions, phototrophic microorganisms tend to colonize mainly calcareous materials and preferentially stuccos over mortars. This is probably due to the chemical availability of calcium from soluble carbonate that can be a source for cyanobacterial sheath formation (Ariño et al. 1997). Therefore, the bioreceptivity of different materials to phototrophic microbial colonization may be ranked as follows: Stucco ≥ mortar > coarse and fine tuff > brick. The observed lower colonization of mortars when compared with stuccos can be related with the high concentration in copper (average value of 174 ppm) that could act as toxic element. Ambient Cu concentrations are toxic to some cyanobacteria probably as a result of non-functional Cu substitution for essential metals (Morel and Price, 2003).

Different microbial species were detected in every biofilm type tested. Two different communities forming green biofilm and white biofilm were observed. Sometimes less extensive darker brownish biofilms were found related with the green ones. Green biofilms showed the highest microbial diversity among the biofilm types; seven cyanobacteria and at least eleven bacteria genera were detected. Brown biofilm diversity was similar to the green ones. White biofilms, however, presented the highest abundance of actinobacteria genera. Previous methodologies based on the culture of microorganisms did not permit the detection of some of these microbial species due to the inability to provide them with appropriate conditions for their growth (Laiz et al. 2003). In fact, previous studies (Albertano and Urzì, 1999) reported that the most frequently encountered cyanobacteria were *Eucapsis, Leptolyngbya, Scytonema* and *Fischerella*. In this study, using molecular techniques, species of the genera *Scytonema*, *Cyanothece*, *Hallospirulina*, *Phormidium*, *Cyanobacterium*, *Aphanothece*, *Gloeothece, Synechococcus, Leptolyngbya* and *Nitrospira* were detected. Although molecular techniques have shown to be highly effective detecting microbial communities and changes between different environmental conditions (Schabereiter-Gurtner et al. 2002; Laiz et al. 2003), a complete correspondence between isolated microorganisms and those detected using molecular techniques was not obtained.

In a separated paper, Saarela et al. (2004) reported the composition of the same biofilms studied here using culturing methodologies. Filamentous actinobacteria, *Streptomyces* spp. were the most common bacteria in biofilm samples. The occurrence of proteolytic bacteria from the genera *Microbacterium*, *Micrococcus*, and *Pseudomonas* was sporadic. Gram-negative slime forming bacteria belonging to the genera *Bosea, Enterobacter, Pectobacter*, *Pseudomonas*, *Sinorhizobium* and *Stenotrophomonas* were also isolated. Fungi, mainly *Acremonium bacillosporum*, *Beauveria alba*, *Lacanicillium* spp. and a *Torrubiella* sp., were more dominant in samples taken from Domitilla than in samples from Saint Callixtus Catacombs. All these isolates were also retrieved from air samples. The different biofilm spectrum when compared with non-cultured analyses (Figure 7) suggests that the cultured strains likely derive from airborne spores.

Culture-dependent and independent techniques generally show disparity of results. Recent studies of the microbial communities from wall paintings using culture-dependent (Heyrman et al. 1999; Saiz-Jimenez and Laiz, 2000) and culture-independent (Rölleke et al. 1996; Schabereiter-Gurtner et al. 2001a) techniques have shown that the culturable microorganisms do not account for the high molecular diversity found in the samples (Rölleke et al. 1996; Schabereiter-Gurtner et al. 2001a, 2002).

Currently, there is debate on understanding the results obtained from diverse analyses using culture-dependent and -independent techniques (Santegoeds et al. 1996; Casamayor et al. 2000; Smit et al. 2001). While culturing methods just give information on the microorganisms able to grow on the culture media used in the experiment, molecular techniques provide with an estimate of the sequences of DNA extracted and amplified from the samples. At present, there is no consensus

on how to relate and complement these results. Culturing techniques are unable to provide with the whole microbial community in a sample for a number of reasons and among them one could underline that (i) we do not know every microbial species present in a sample, (ii) the ideal conditions allowing growth of each of the microorganisms in a sample is also unknown, and (iii) some of the microbes in a sample could be in dormant physiological stages and might not show growth using standard culturing procedures.

Culturing-independent techniques ideally can allow us to know the microbial community present in a sample, which clearly complements culturing techniques. However, molecular methods do not provide any information on the physiological stage of the detected microbes; these microorganisms could be actively growing, viable, dormant, or they could have even died and their DNA might still be present in the sample. Besides, culture-independent techniques require optimisation in order to obtain a maximum information from the processed samples.

Laiz et al. (2003) prepared an experimental system to analyse the possible biases involved in studies of microbial communities in monuments using either culture-dependent and -independent techniques and the possible pitfalls associated to these methodologies. A consortium composed by 14 microbial species was inoculated in building materials and incubated for six months. The microorganisms used in their experiments have been reported to be able to produce damage on monuments, such as staining, discoloration, patinas, and efflorescences (Gurtner et al. 2000; Schabereiter-Gurtner et al. 2001b). In these experiments, only 5 out of 14 strains could be cultivated after 6 months incubation on building materials. The cultured species were mostly Gram-positive, spore-forming species (i.e., *Bacillus*) suggesting that these strains were detected because of their ability to form spores. The same can be applied to species of *Streptomyces*, the most commonly found isolated in the catacombs. By a culture-independent technique the presence of the inoculated species was detected in the samples.

Since in the experiment was used an inoculum of known composition and all strains proved to grow in the culture media used, Laiz et al. (2003) stated they should be able to recover these species if they were in a viable physiological stage. This ruled out the possibility that differences between culture-dependent and -independent techniques was a result of using inadequate culture media or incubation conditions. Consequently, comparing culturing and molecular results, it was deduced that the ability to retrieve some of the inoculated species was a consequence of their ability to form spores and the unculturable species were under dormant physiological stages of survival or lysed after a prolonged incubation, including natural dryness periods.

Condensation processes are highly remarkable in catacomb visited areas and give rise to ceilings coverage by drops of water or a water thin layer. It is due to high relative humidity close to 95-100% and the lower temperature of materials with respect to air temperature. Water condensation is usually present in many different surfaces but mainly on highly porous and rough volcanic rock, where biofilm

development is extremely large. We suggest that textural features, such as the porosity, are also critical factors in biofilm colonization. Volcanic tuff showed higher roughness than building materials, which favoured microbial adhesion. For example, many bricks or marbles remain encrusted on walls and tombstones and condense a lot of water, but not much biofilm development is observed. High-porosity values allow deep penetration of moisture into the material preparing suitable conditions for the settlement of rock-colonising microorganisms. The availability of water in each material is a critical factor for microbial colonisation and depends directly on the characteristic of its porous system. The presence of an extensive inner pore surface, resulting from a high porosity or the presence of clay minerals, facilitates the spreading of microorganisms within the pore system (Warscheid and Braams, 2000).

An important parameter that describes the porous media of materials is the specific surface area (SSA) that is also directly related to porosity and inversely related to pore size, and quantifies the surface exposition of material to be decayed (Gregg and Sing, 1982). Moreover, SSA plays an important role in the condensation process on porous materials since it is inversely related to pore size. Consensation is particularly strong in pores with a radius lower than 0.1 μm when the Kelvin effect dominates. Thus, material with high values of SSA implies a high capacity and susceptibility of water condensation and retention into the materials. Microorganisms showing low tolerance to desiccation and water stress than cyanobacteria usually developed far from the lamps. These form white biofilms that are related with high water availability. As we could observe, wet areas are located in corridor ceilings as water holds more easily on volcanic tuff surfaces. It means a relation between human breathing, air temperature, high relative humidity and type of material. White biofilm shows the following rank of material preference: Fine tuff > coarse tuff > mortar > stucco > brick. This sequence is in complete agreement to the values of SSA measured for each material type (Table 1).

To summarize, changes induced by visitors favour material decay. This can be observed in areas around lamps which suffer strong environmental changes daily, involving: (i) a high increase of air and material surface temperature induced by the lamps, as the surface can reach 40°C; (ii) the evaporation of available water and the decrease of air relative humidity raising the saturation water vapour pressure in the air; (iii) total air humidity and CO_2 air concentration increases induced by visitors; (iv) rapid decrease of temperature when turning off the lamp causing fast condensation processes of CO_2-enriched acid water on materials and biofilms; (v) micro-corrosion of calcareous materials (stuccos) dissolving soluble minerals (e.g. calcite) and increasing both availability of nutrients and surface roughness.

The long term chemical alteration of the volcanic rock favours its softness and friability. The mechanical differences between the volcanic rock and the building materials produce wall flacking. In addition, aesthetic deterioration was observed due to biofilm coverage of mural paintings. Biofilms coating walls represent a great aesthetic impact, both green coloured around the lamps and the white ones on corridors and ceilings.

As a consequence of this study, an appropriate lighting strategy for controlling phototrophic biofilms is needed. Albertano and Bruno (2003) proposed the use of a combination of green and/or red light since utilizing these zones of the visible spectrum very few photosynthetic organisms, if any, will be able to grow. The set up of an illumination system able to minimize cyanobacterial growth and temperature increases are one of the urgent countermeasures to be adopted in order to protect hypogean cultural heritage from deterioration.

Acknowledgements

This work was supported by the European Commission, project EVK4-CT2000-00028 and the Spanish Ministry of Education and Science, project BTE2002-04492-C02. LL and JMG benefit from European Social Fund and Ramón and Cajal contracts, respectively.

References

Albertano P, Bruno L. The importance of light in the conservation of hypogean monuments. In: Saiz-Jimenez C, editor. Molecular Biology and Cultural Heritage, Balkema, Lisse, 2003, pp. 171-177.

Albertano P, Urzì C. Structural interactions among epilithic cyanobacteria and heterotrophic microorganisms in Roman hypogea. Microb Ecol 1999; 38: 244-252.

Albertano P, Moscone D, Palleschi G, Hermosin B, Saiz-Jimenez C, Sanchez-Moral S, Hernandez-Marine M, Urzì C, Groth I, Schroeckh V, Saarela M, Mattila-Sandholm T, Gallon JR, Graziottin F, Bisconti F, Giuliani R. Cyanobacteria attack rocks (CATS): Control and preventive strategies to avoid damage caused by cyanobacteria and associated microorganisms in Roman hypogean monuments. In: Saiz-Jimenez C, editor. Molecular Biology and Cultural Heritage, Balkema, Lisse, 2003, pp. 151-162.

Altschul SF, Gish W, Miller W, Myers EW, Lipman DJ. Basic local alignment search tool. J Mol Biol 1990; 215: 403-410.

Ariño X, Saiz-Jimenez C. Factors affecting the colonization and distribution of cyanobacteria, algae and lichens in ancient mortars. In: Riederer J, editor. Proceedings of the 8th International Congress on Deterioration and Conservation of Stone. Möller, Berlin, 1996, vol. 2, pp. 725-731.

Ariño X, Hernandez-Marine M, Saiz-Jimenez C. Colonization of Roman tombs by calcifying cyanobacteria. Phycologia 1997; 36, 366-373.

Buczynski C, Chafetz HS. Habit of bacterially induced precipitates of calcium carbonate and the influence of medium viscosity on mineralogy. J Sedim Petrol 1991; 61: 226-233.

Casamayor, EO, Schäfer H, Bañeras L, Pedròs-Aliò C, Muyzer G. Identification of and spatio-temporal differences between microbial assemblages from two neighbouring sulphurous lakes: comparison by microscopy and denaturing gradient gel electrophoresis. Appl. Environ. Microbiol 2000; 66: 499-508.

Ehrlich HL. Geomicrobiology: its significance for geology. Earth-Sci Rev 1998; 45: 45-60.

Edwards U, Rogall T, Blöcker H, Emde M, Böttger EC. Isolation and direct complete nucleotide determination of entire genes. Characterization of a gene coding for 16S ribosomal RNA. Nucleic Acids Res 1989; 17: 7843-7853.

Gonzalez JM, Ortiz-Martinez A, Gonzalez-delValle MA, Laiz L, Saiz-Jimenez C. 2003. An efficient strategy for screening large cloned libraries of amplified 16S rDNA sequences from complex environmental communities. J Microbiol Meth 2003; 55: 459-463.

Gregg SJ, Sing KSW. Adsorption, Surface Area, and Porosity. Academic Press, London 1982.

Guillitte O. Bioreceptivity: a new concept for building ecology studies. Sci Total Environ 1995; 167: 215-220.

Gurtner C, Heyrman J, Piñar G, Lubitz W, Swings J, Rölleke S. Comparative analyses of the bacterial diversity on two different biodeteriorated wall paintings by DGGE and 16S rDNA sequence analysis. Int Biodeter Biodegr 2000; 46: 229-239.

Heyrman J, Mergaert J, Denys R, Swings J. The use of fatty methyl ester analysis (FAME) for the identification of heterotropic bacteria present on three mural paintings showing severe damage by microorganisms. FEMS Microbiol Lett 1999; 181: 55-62.

Keinänen MM, Korhonen LK, Lehtola MJ, Miettinen IT, Martikainen PJ, Vartiainen T, Suutari MH. The microbial community structure of drinking water biofilms can be affected by phosphorus availability. Appl Environ Microbiol 2002; 68: 434-439.

Laiz L, Piñar G, Lubitz W, Saiz-Jimenez C. Monitoring the colonization of monuments by bacteria : cultivation versus molecular methods. Environ Microbiol 2003; 5: 72-74.

Morel FMM, Price NM. The biogeochemical cycles of trace metals in the oceans. Science 2003; 300: 944-947.

Muyzer G, de Waal EC, Uitterlinden AG. Profiling of complex microbial populations by denaturing gradient gel electrophoresis analysis of polymerase chain reaction-amplified genes coding for 16S rRNA. Appl Environ Microbiol 1993; 59: 695-700.

Nübel U, Garcia-Pichel F, Muyzer G. PCR primers to amplify 16 rRNA genes from cyanobacteria. Appl Environ Microbiol 1997; 63: 3327-3332.

Rölleke S, Muyzer G, Wawer C, Wanner G, Lubitz W. Identification of bacteria in a biodegraded wall painting by denaturing gradient gel electrophoresis of PCR-amplified gene fragments coding for 16S rRNA. Appl Environ Microbiol 1996; 62: 2059-2065.

Saarela M, Alakomi H-L, Suihko M-L, Maunuksela L, Raaska L, Mattila-Sandholm T. Heterotrophic microorganisms in air and biofilm samples from Roman catacombs, with special emphasis on actinobacteria and fungi. Int Biodeter Biodegr 2004; 54, 27-37.

Saiz-Jimenez C, Laiz L. Occurrence of halotolerant/halophilic bacterial communities in deteriorated monuments. Int Biodeter Biodegr 2000; 46: 319-326.

Sanchez-Moral S, Bedoya J, Luque L, Cañaveras JC, Jurado V, Laiz L, Saiz-Jimenez C. Biomineralization of different crystalline phases by bacteria isolated from catacombs. In: Saiz-Jimenez, C. editor. Molecular Biology and Cultural Heritage. Balkema, Lisse, 2003a; pp.179-185.

Sanchez-Moral S, Cañaveras JC, Laiz L, Saiz-Jimenez C, Bedoya J, Luque L. Biomediated precipitation of calcium carbonate metastable phases in hypogean environments. A short review. Geomicrobiology Journal 2003b; 20: 491-500.

Sanchez-Moral S, Luque L, Cañaveras JC, Laiz L, Jurado V, Hermosin B, Saiz-Jimenez C. Bioinduced barium precipitation in Saint Callixtus and Domitilla Catacombs. Ann Microbiol 2004a; 54: 1-12.

Sanchez-Moral S, Luque L, Cuezva S, Soler V. Environmental changes induced by visitors in the Roman catacombs of St. Callixtus (Rome, Italy). In: Saiz-Jimenez, C. editor. Air Pollution and Cultural Heritage. Balkema, Leiden, 2004b, pp. 183-190.

Santegoeds CM, Nold SC, Ward DM Denaturing gradient gel electrophoresis used to monitor the enrichment culture of aerobic chemoorganotrophic bacteria

from a hot spring cyanobacterial mat. Appl. Environ. Microbiol 1996; 62: 3922-3928.

Schabereiter-Gurtner C, Saiz-Jimenez C, Piñar G, Lubitz W, Rölleke S. Altamira cave paleolithic paintings harbor partly unknown bacterial communities. FEMS Microbiol Lett 2002; 211: 7-11.

Schabereiter-Gurtner C, Piñar G, Lubitz W, Rölleke S. An advanced molecular strategy to identify bacterial communities on art objects. J Microbiol Meth 2001a; 45: 77-87.

Schabereiter-Gurtner C, Piñar G, Vybiral D, Lubitz W, Rölleke S. Rubrobacter-related bacteria associated with rosy discoloration of masonry and lime wall paintings. Arch Microbiol 2001b; 176: 347-354.

Smit E, Leeflang P, Gommans S, van den Broek J, van Mil S, Wernars K. Diversity and seasonal fluctuations of the dominant members of the bacterial soil community in a wheat field as determined by cultivation and molecular methods. Appl Environ Microbiol 2001; 67: 2284-2291.

Warscheid Th, Braams J. 2000. Bioreceptivity of building stones. Int Biodeter Biodegr 2000; 46: 343-368.

Figure Captions

Figure 1. Saint Callixtus Catacombs (Crypt of La Pecorelle) showing the main different types of materials: A) Tuff, B) Mortar, C) Stucco, D) Brick.

Figure 2. Left) A section of building materials. A: Fine tuff, B_1: Coarse mortar, B_2: Fine mortar and C: Stucco coating volcanic host rock. Right) Different textures of volcanic rocks.

Figure 3. Thin sections showing petrographic characteristics of different materials. A) Contact between stucco and mortar. Note the different texture of materials and the high pore size in stucco related with retraction fissures. B) Contact between mortar and fine-grained tuff. Note the thin layer of micritic calcite extended onto the contact surface.

Figure 4. Environmental scanning electron micrographs showing different details of biofilms. A) External surface of green biofilm. B) Calcite precipitation around cyanobacteria sheaths. C) Section showing thin green biofilm, separated from the stucco surface. Note the abundant diatoms. D) Detail of a green biofilm formed by cyanobacteria and actinobacteria. E) Section showing white biofilm with a dense net of needle-like calcite crystals. F) Detail of the external surface of white biofilm. G) Details of filaments in the internal area of white biofilm close to the surface. Note the calcium carbonate nucleation points. H) Detail of the inner part of white biofilm showing spherical particles associated with needle-fiber calcite crystals and beaded filaments.

Figure 5. Microclimatic data from San Callixtus Catacombs: A) Annual cycles of air temperture, CO_2 concentration and humidity, B) Three days record of air temperature, CO_2 concentration, and soil temperature -lower than air temperature during the whole daily cycle.

Figure 6. Sketch of a catacomb's crypt and corridor showing biofilm distribution: A) Green biofilm, B) White biofilm.

Figure 7. Detail of ethidium bromide-stained 16S rDNA DGGE community fingerprints of samples 15A (A), 16A (B) and CR-B (C) from green biofilms; 15E (D) and 16D (E) from white biofilms; and 15B (F) and 16B (G) from brown biofilms. Band identification corresponded to sequenced and phylogenetically analyzed clones, In addition, species detected, but unlocalized on the DGGE community fingerprints, were for the green biofilm: *Gloeothece* sp., two uncultured cyanobacteria, *Cyanothece* sp., uncultured *Aphanotece*, and three uncultured bacteria; for the white biofilm: *Cyanobacterium*, *Cyanothece*, *Leptolynbya*, uncultured *Planctomycetes*, delta-Proteobacterium, *Lyngbya majuscula,* two uncultured cyanobacteria, alpha-Proteobacterium, and gamma-Proteobacterium; and for the brown biofilm: Uncultured *Cyanobacterium*, and uncultured bacterium. Underlined species in the fingerprints correspond to the *Cyanobacteria*.

Table 1. Mean of chemical composition, mineral composition and porosity of five material types

MAJOR ELEMENTS	Coarse Tuff	Fine Tuff	Mortar	Stucco	Brick
SiO_2	44.58	46.98	36.87	33.55	49.2
TiO_2	0.65	0.71	0.43	0.43	0.55
Al_2O_3	18.39	19.36	13.35	11.20	14.89
Fe_2O_3	6.57	7.49	4.50	2.69	6.41
FeO	1.33	1.04	1.30	1.83	0.56
MnO	0.19	0.29	0.17	0.10	0.14
MgO	2.42	2.15	2.31	1.62	2.66
CaO	8.61	4.75	17.10	21.78	14.33
Na_2O	4.00	0.93	2.12	1.83	1.38
K_2O	1.12	3.16	1.46	0.89	2.02
P_2O_5	0.23	0.19	0.18	0.36	0.29
P. C.	11.89	12.64	19.93	23.30	7.36
TRACE ELEMENTS					
Sr	988	1219	962	948	-
Ba	1940	2816	1434	2317	-
Pb	138	124	196	244	-
Cr	17	47	19	20	-
Co	17	19	14	16	-
Ni	24	32	28	33	-
Cu	40	47	174	59	-
Zn	67	72	50	52	-
Mo	0.25	0.40	0.28	0.45	-
MINERAL					
Phyllosilicates	50	78	33	14	24
Pyroxene	15	5	11	7	6
Feldspar	4	6	3	0	33
Analcime	25	2	15	17	0
Calcite	3	1	41	51	16
Others	<3	<8	<2	<1	<25
POROSITY					
SSA [m^2/g]	32.71	78.27	38.92	6.61	1.92
ρ_{true} [g/cm^3]	4.215	2.819	3.223	3.076	3.288
P_{conc} [%]	50.36	36.39	45.86	28.15	42.99
r_m [µm]	1.116	0.020	0.130	1.129	0.379
ρ_{bulk} [g/cm^3]	1.271	1.498	1.217	1.937	1.499
P_T [%]	69.84	46.85	62.31	37.04	54.40

Table 2.- Biofilm type and distribution as a function of material type, distance to lamps (L) and condensation rate. G: Green biofilm. W: White biofilm. B: brown biofilm. N: No biofilm. Bold capital letters (**G, W**) indicate major occurrence, normal capital letters (G, W, N) represent medium incidence and low-case letters (g, w) imply minor development.

	L<0.6-0.8m	L>0.8m	
		Induced condensation	Low/No condensation
coarse tuff	g	W	w/N
fine tuff	g+w	**W**	w/N
mortar	G+b	w	N
stucco	**G**+B	w	N
brick	<g	<w	N

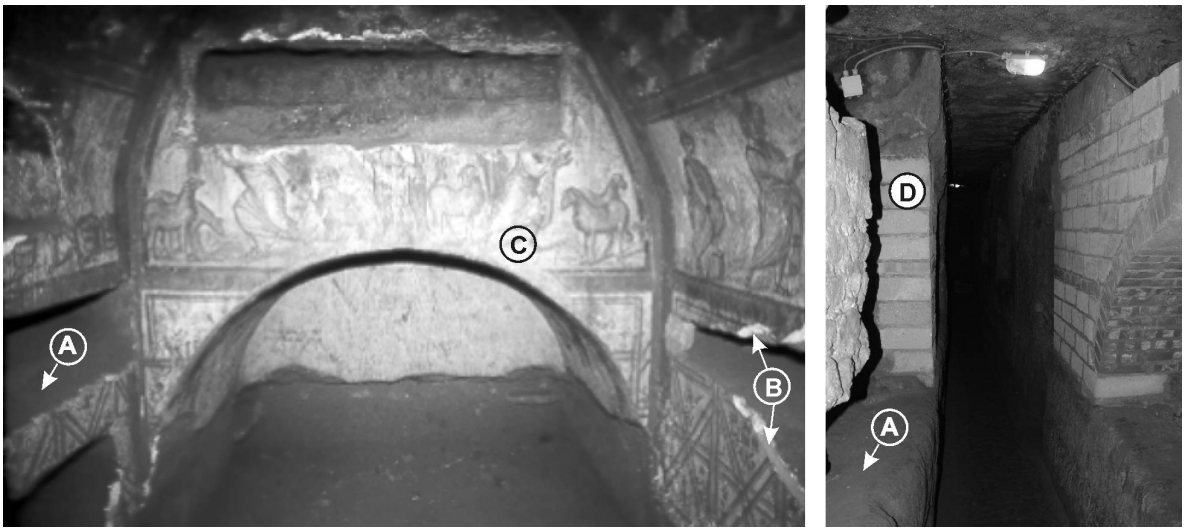

Figure 1

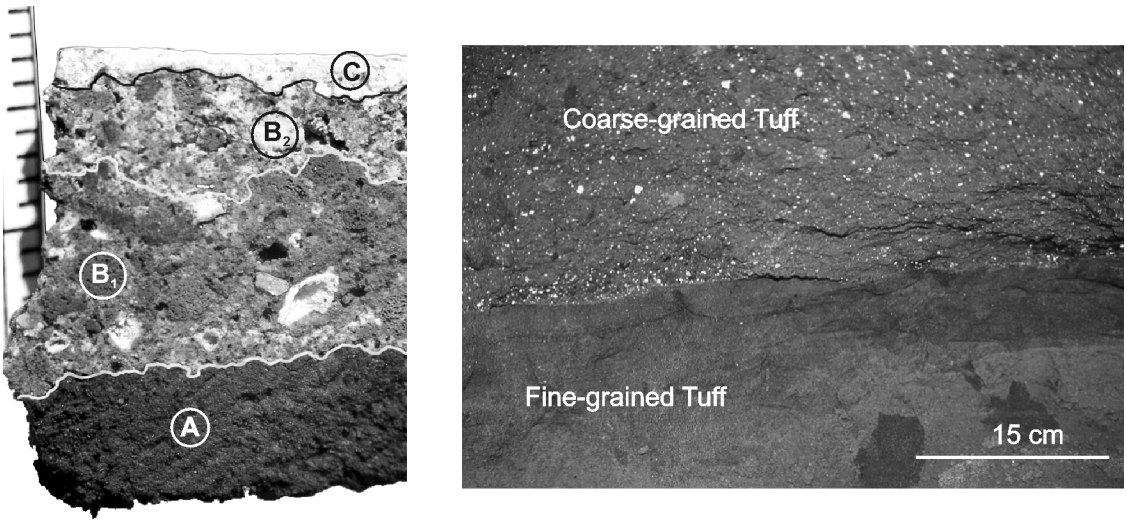

Figure 2

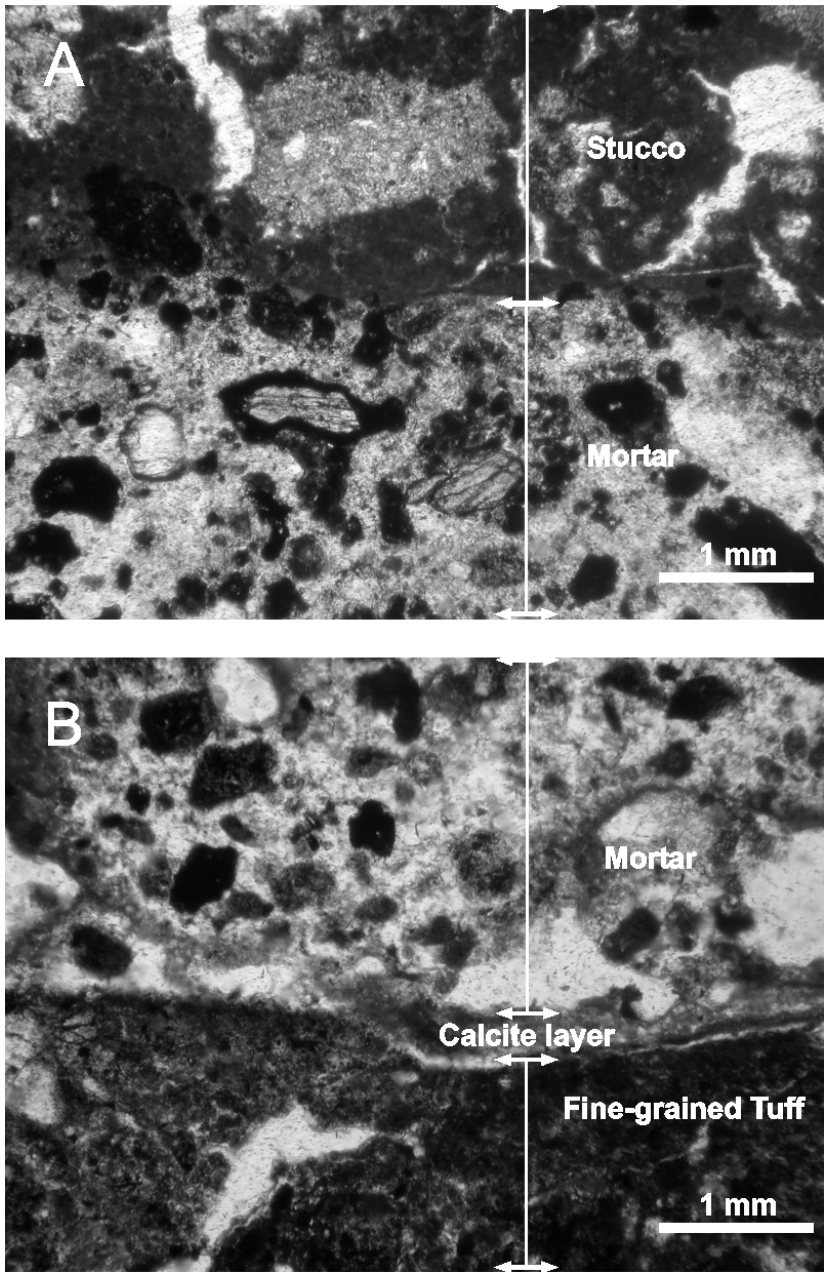
A
Stucco
Mortar
1 mm
B
Mortar
Calcite layer
Fine-grained Tuff
1 mm

Figure 3

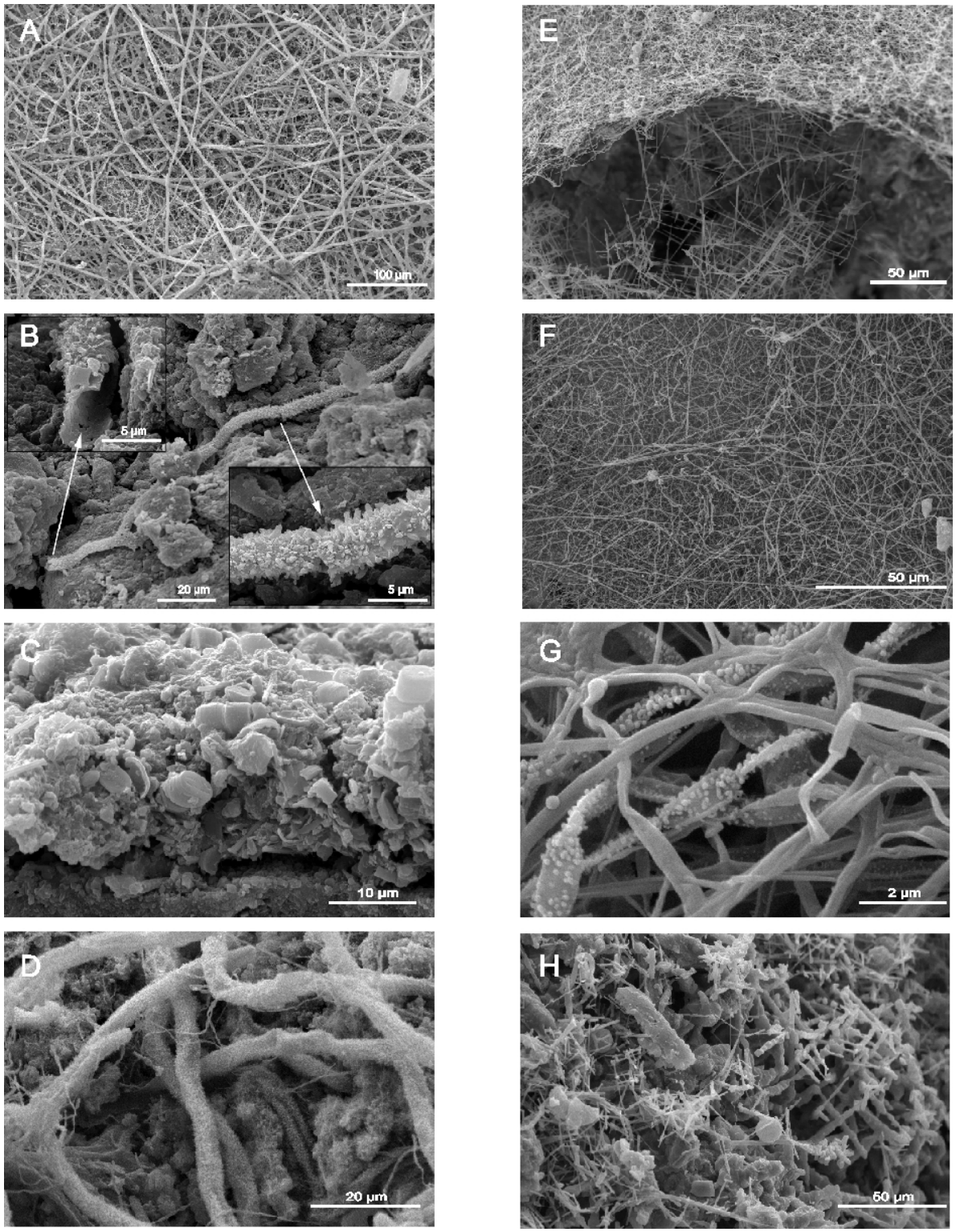

Figure 4

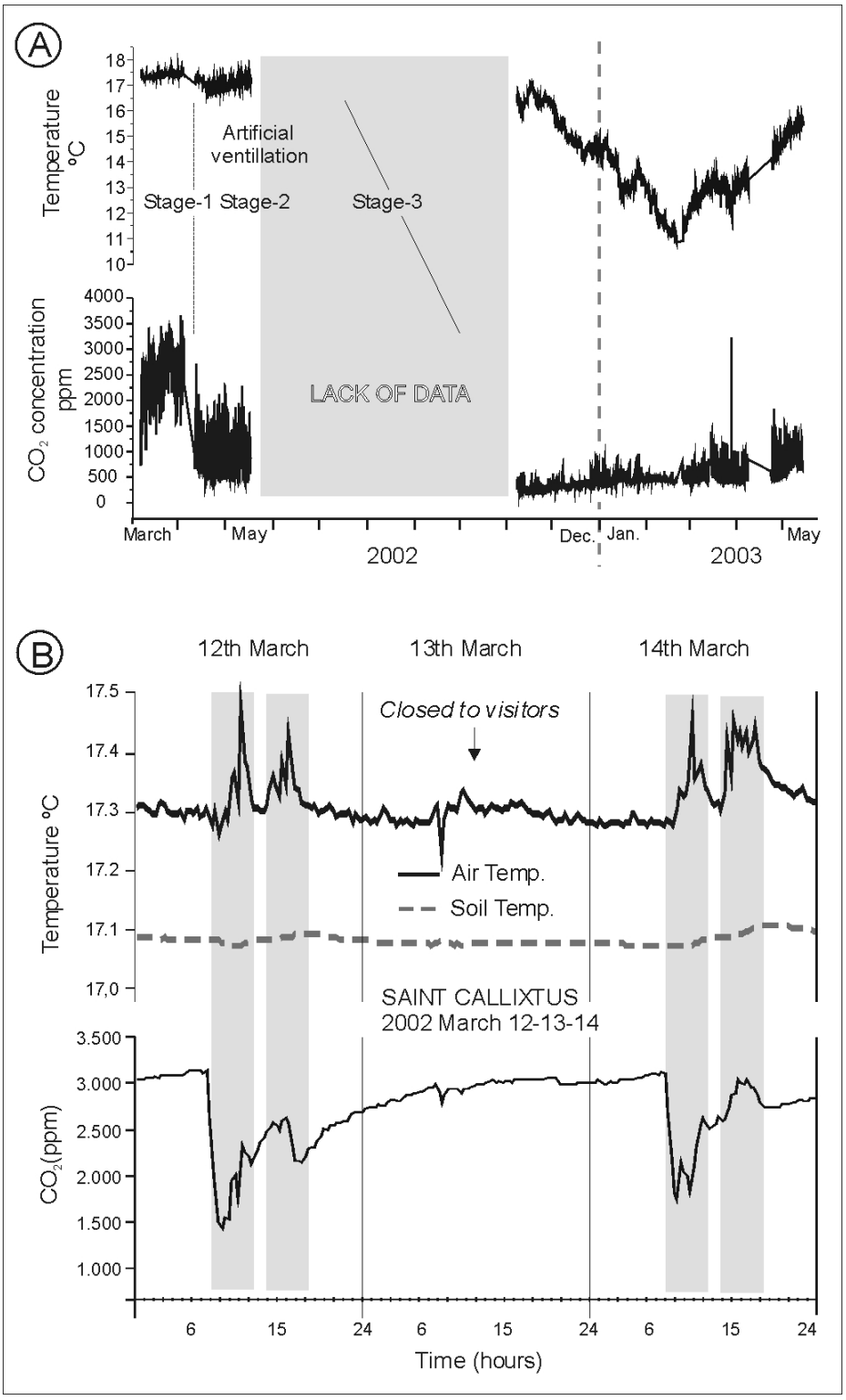
A
Temperature °C
18
17
16
15
14
13
12
11
10
Artificial ventillation
Stage-1
Stage-2
Stage-3
CO2 concentration ppm
4000
3500
3000
2500
2000
1500
1000
500
0
LACK OF DATA
March
May
2002
Dec.
Jan.
May
2003
B
12th March
13th March
14th March
Temperature °C
17.5
17.4
17.3
17.2
17.1
17,0
Closed to visitors
Air Temp.
Soil Temp.
SAINT CALLIXTUS
2002 March 12-13-14
CO2(ppm)
3.500
3.000
2.500
2.000
1.500
1.000
6
15
24
6
15
24
6
15
24
Time (hours)

Figure 5

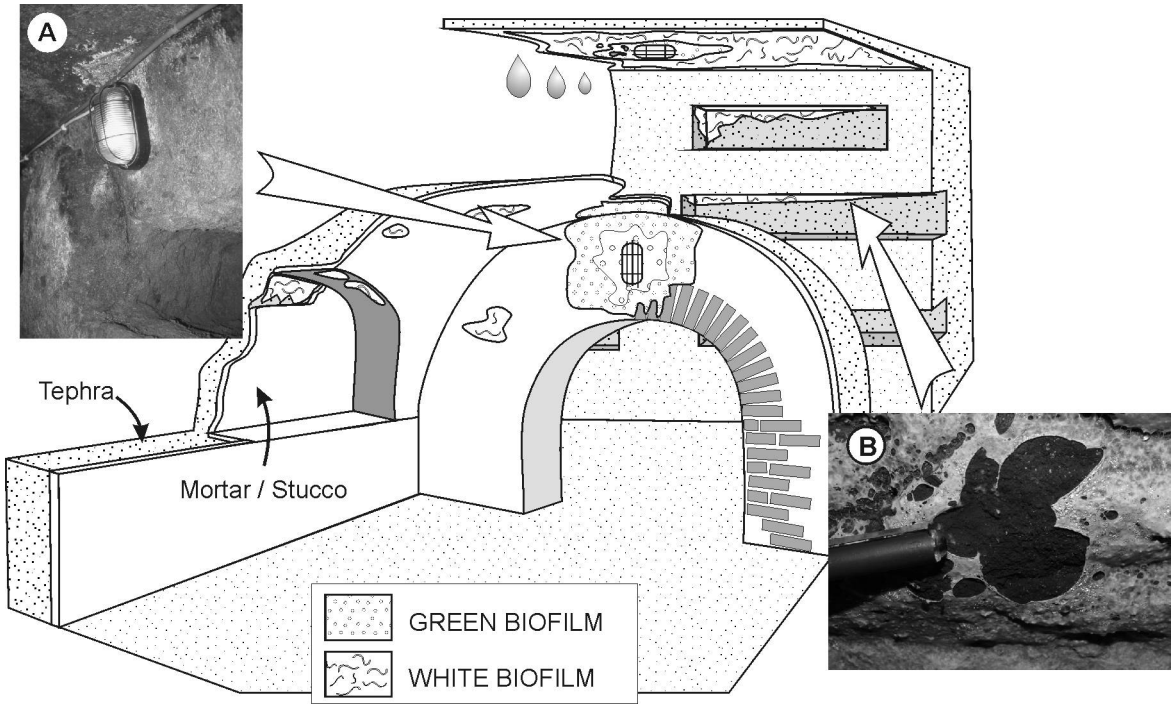

Figure 6

Figure 7

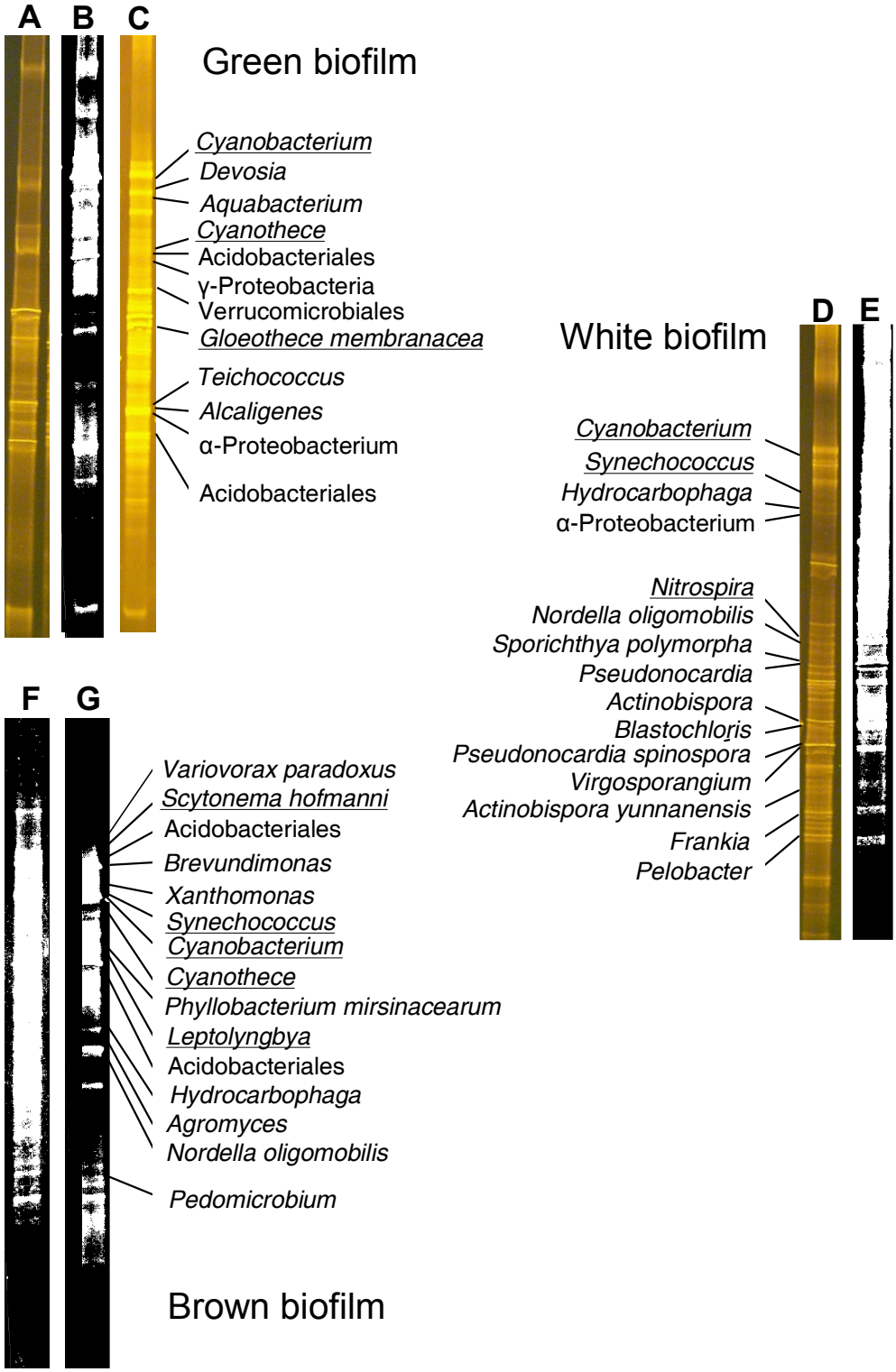
A
B
C
Green biofilm
Cyanobacterium
Devosia
Aquabacterium
Cyanothece
Acidobacteriales
γ-Proteobacteria
Verrucomicrobiales
Gloeothece membranacea
Teichococcus
Alcaligenes
α-Proteobacterium
Acidobacteriales
D
E
White biofilm
Cyanobacterium
Synechococcus
Hydrocarbophaga
α-Proteobacterium
Nitrospira
Nordella oligomobilis
Sporichthya polymorpha
Pseudonocardia
Actinobispora
Blastochloris
Pseudonocardia spinospora
Virgosporangium
Actinobispora yunnanensis
Frankia
Pelobacter
F
G
Variovorax paradoxus
Scytonema hofmanni
Acidobacteriales
Brevundimonas
Xanthomonas
Synechococcus
Cyanobacterium
Cyanothece
Phyllobacterium mirsinacearum
Leptolyngbya
Acidobacteriales
Hydrocarbophaga
Agromyces
Nordella oligomobilis
Pedomicrobium
Brown biofilm